and HCV-OC43, which are known to be heavily glycosylated and detected at 186 kDa and 190 kDa, respectively (17). Our result is consistent with the data reported recently by Xiao *et al.* who expressed the full-length S glycoprotein of SARS-CoV Tor2 strain in 293 cells and showed that the protein ran ~180–200 kDa in SDS gels (18). The origins of the 120 kDa and the faint 37 kDa bands were unknown. However, similar bands were also detected on a fluorogram by using anti-N mAbs (Ohnishi, K., Sakaguchi, M., Takasuka, N. *et al.*, unpublished data), suggesting that it is related to N protein. The specificity of IgG in the immune sera was also determined by ELISA plates coated with lysates of cells infected with either S- or N-expressing recombinant vaccinia viruses (Fig. 4B). The results indicated that anti-S as well as anti-N protein IgG antibodies were elicited by virion/alum vaccination.

Table I. Neutralizing activity in serum after vaccination

		Reciprocal endpoint titer	
		Experiment 1	Experiment 2
None/alum		<5*	<5*
Virion	mouse 1	250	250
	2	1250	250
	3	1250	250
Virion/alum	1	250	1250
	2	1250	1250
	3	1250	1250

*All six mice examined did not have detectable neutralizing activity. Sera were obtained from mice 1 week after boost vaccination and subjected to SARS-CoV neutralizing activity assay as described in Methods. The titer is a reciprocal number of minimum serum dilution that inhibits the cytopathic effect.

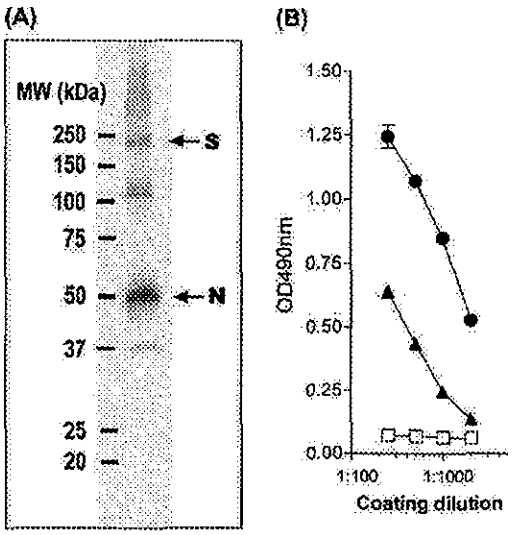

Fig. 4. Specificity of the serum antibodies. (A) Purified UV-inactivated SARS-CoV virion (0.5 μg) was fractionated by SDS–PAGE and subjected to western blotting. Diluted pooled sera (1:1000) from mice primed and boosted with virion/alum were exploited to detect virus proteins. Upper and lower arrows indicate the predicted band of S (spike protein) and N (nucleocapside protein) of SARS-CoV, respectively. The size of molecular weight markers (kDa) is shown on the left. (B) S protein- or N protein-specific ELISA. ELISA plates were coated at the indicated dilution with 1% NP40 lysates of chick embryo fibroblasts that had been infected with S protein-expressing vaccinia virus (circle), N protein-expressing vaccinia virus (triangle) or uninfected (mock; square). Diluted serum (1:1000) from mice prime and boost immunized with virion/alum, was exploited for detection of virus proteins.

UV-inactivated SARS-CoV whole virion induces T-cell response

To examine whether or not subcutaneously vaccinated mice gained an induced T-cell response against SARS-CoV, mice were immunized either with virion/alum, virion, or alum only via the footpad. T cells of these mice were enriched from the spleen and regional lymph nodes 1 week after a booster immunization and cultured with irradiated APCs in the presence or absence of UV-inactivated SARS-CoV virion at 1 or 10 μg/ml. As shown in Fig. 5(A), regional lymph node T cells proliferated *in vitro* in response to UV-inactivated virion in virion/alum-immunized mice and, to a lesser extent, in virion-immunized mice. Because mice inoculated with virion/alum showed a high basal level of proliferation of lymph node T cells in the absence of antigen, there is not much difference in the net proliferative response of these cells between the virion/alum group and the virion only group. On the other hand, in splenic T cells, a low level of proliferation was observed only in the virion/alum group of mice. The level of proliferation of these T cells, however, was virion-dose independent. Therefore, our results suggest that the subcutaneous injection of inactivated virion, even without alum, does induce T cell activation to some extent in the draining lymph node, a result which hardly occurs systemically.

We also measured the level of cytokine production in the supernatant of lymph node T cells stimulated with inactivated virion *in vitro* for 4 days. We found that the inactivated virion induced the production of all the cytokines (IL-2, IL-4, IL-5, IFN-γ and TNF-α) in T cells of virion/alum-immunized mice, in a dose-dependent manner (Fig. 5B). Likewise, T cells of virion-immunized mice produced low, yet significant, levels of these cytokines in a dose-dependent manner, except IL-5. In contrast, lymph node T cells from normal mice did not produce any cytokines at all in response to virion, suggesting that the virion itself does not possess innate stimulating activity as bacterial products [such as lipopolysaccharide (LPS) and purified protein derivative of mycobacterium tuberculosis (PPD)] do. Taken together, these results suggest that subcutaneous vaccination with UV-inactivated SARS-CoV is able to activate $CD4^+$ T cells in regional lymph nodes, where T cells produce several immunoregulatory cytokines, including IFN-γ.

Discussion

The present results demonstrated that even a single subcutaneous administration of UV-irradiated virion without alum adjuvant induced a high level of systemic anti-SARS-CoV antibody response in mice, probably followed by the generation of long-term antibody-secreting cells and memory cells in the bone marrow. Considering that polyvalent particulate

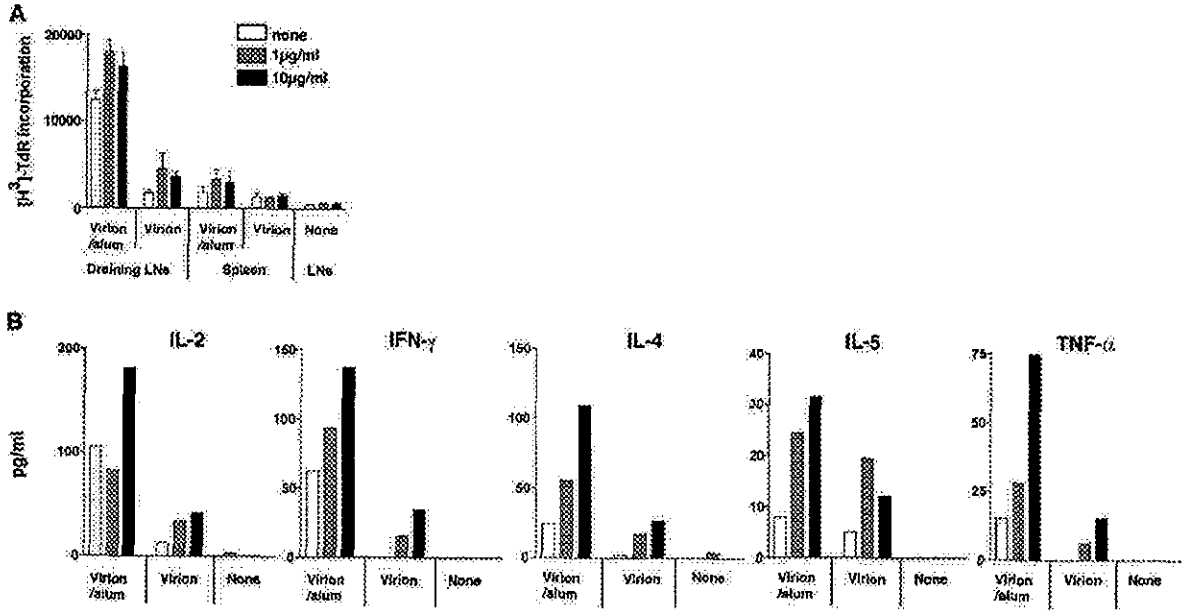

Fig. 5. *In vitro* responses of SARS-CoV-specific T cells taken from mice vaccinated with inactivated SARS-CoV. Mice were subcutaneously primed with 10 μg of UV-inactivated SARS-CoV virion, or virion with 2 mg of alum, or none, and then boosted with the same dose in their footpads at 7 weeks after priming. Draining lymph nodes and spleens were isolated at 1 week after boost and stimulated with T-cell depleted splenocytes that had been pulsed with the indicated concentration of UV-inactivated SARS-CoV virion. These cells were cultured for 2–4 days and [^{3}H]thymidine was added 8 h prior to the harvest. The peak response on day 4 after cultivation is shown in (A). (B) Culture supernatant was collected at day 2–4 post cultivation and the level of IL-2, IFN-γ, IL-4, IL-5 and TNF-α was determined by CBA kit. The maximum cytokine production at day 4 is shown. Results are representative of two separate experiments.

structures such as hepatitis B virus surface antigen-based, HIV-1 Gag-based and Ty virus-like particles have been shown to elicit humoral as well as cellular immune responses (19), these particulates probably have comparable dimensions and structures to the pathogens that are targeted for uptake by APCs to facilitate the induction of potent immune responses. The antibodies elicited in mice vaccinated by the current protocol with or without adjuvant recognized both the S and N proteins of SARS-CoV and were able to neutralize the infection of virus to Vero E6 cells. However, serum anti-SARS-CoV IgA antibody was not detectable, probably owing to the route of vaccination. In addition, the present vaccination protocol caused T cell response at the regional lymph nodes, although it did not allow for the induction of a sufficient cellular immune response systemically.

We show here the potentiality of subcutaneous injection of inactivated virion with alum, which is utilized for most of current human vaccinations. Alum has been used as an adjuvant for vaccines such as diphtheria, pertussis and tetanus, and these vaccines have a long safety record for human use (20). We observed that the addition of alum to the vaccine formula resulted in a large augmentation of serum IgG_1 production, but not IgG_{2a} production. The level of IgG_1 in alum-vaccinated mice reached a level similar to that found in hyper-immunized mice, which were subcutaneously injected with 5 μg of inactivated virion emulsified with a complete Freund adjuvant, followed by consecutive three-times intravenous boosters with 2 μg of virion. Alum is known to selectively stimulate an IgG_1 dominant, type 2 immune response [reviewed in (21)]. Activation of complement by alum could contribute to the type 2-biased immune response partly via an inhibition of IL-12 production. Interestingly, a quite recent report demonstrated that an alum-induced $Gr1^+$ myeloid cell population produced IL-4 and activated B-cells (22).

There are various diseases associated with animal coronavirus infection. The clinical manifestations of the disease and the correlates of protection with immunity have been studied extensively in these animal coronavirus infections [reviewed in (7)]. Although antibodies and T cells may play a role in exacerbating the pathology in some animal coronavirus infections (23,24), both humoral and cellular immune responses are known to contribute to protection against coronavirus infection. In murine hepatitis virus, a Group 2 coronavirus, the mortality of susceptible mice was partially prevented by the transfer of immune serum containing neutralizing antibody prior to challenge (25). Recently, Zhi-yong *et al.* reported in the murine acute infection model that the neutralizing antibody elicited by vaccination of DNA encoding S was protective, but cellular components of vaccinated mice were not required for the inhibition of viral replication (26). Because a twice parenteral administration of inactivated virion with alum induced a high level of antibodies that are able to neutralize SARS-CoV, this vaccination protocol may have a certain effect on the protection of humans from SARS-CoV infection.

We observed that two successive inoculations with inactivated virus at 7 week intervals generated SARS-CoV-specific

T cells. These cells were restimulated with the irradiated virus *in vitro*, but their response was low in terms of the level of proliferation and production of INF-γ and IL-2. However, irrespective of vaccination protocols with or without alum adjuvant, virus-primed T cells of vaccinated animals were capable of producing IL-4 at high levels upon *in vitro* stimulation, comparable to other reports for a variety of vaccination studies (27,28). This outlook seems compatible with the idea that the present vaccine protocol may tend to select T-cell subsets with Th2 phenotype. However, it remains to be elucidated whether such T cells may exhibit serological memory phenotype and persist in the immune system after vaccination as long as memory B cells, which may persist more than 180 days post vaccination. In addition, further analysis is needed to clarify whether T cell response is a crucial factor for long-term protection against SARS-CoV infections.

Efforts to develop a SARS-CoV vaccine have been carried out by many profitable or non-profitable organizations in various ways. For example, it has recently been reported that the combination of adenovirus vector expressing SARS-S, -M or -N protein elicited a neutralizing capacity in serum and N-specific T-cell response in rhesus macaques (29). However, it is still uncertain whether or not the immunity against only these components of SARS-CoV is sufficient for virus protection. SARS-CoV tends to cause replication errors, which may allow the virus to escape the host-immune response and result in a seasonal outbreak. From this point of view, it resembles influenza virus. In influenza virus, inactivated HA vaccine showed incomplete protection but had a certain efficacy and safety record for a long period of time. Indeed, this approach has been used in the veterinary field, such as with the bovine coronavirus (30) and canine coronavirus (31). These advantages make a whole killed virion a prime candidate for a SARS vaccine, even if it may not have the best protective ability.

Unfortunately, no information is available so far on the immune correlates of protection against human coronaviruses, including SARS-CoV. In consideration that SARS-CoV transmission occurs by direct contact with droplets or by the fecal oral route, mucosal secretary IgA in both the lower respiratory tract and digestive tract seem to be crucially important. Failure to induce IgA-type antibodies in a current systemic vaccination method should be improved. Notably, IgA antibodies were detectable in the sera and bronchoalveolar lavage fluid obtained from mice hyper-immunized with UV-irradiated virus (data not shown). Therefore, if a non-toxic and more potent adjuvant becomes available for human use, the subcutaneous injection of inactivated virion would become an effective vaccination method to reduce the number of susceptible people.

In the future, it will be necessary to determine whether or not the inactivated whole virion vaccine possesses protective ability against SARS-CoV infection by the use of adequate animal models. Furthermore, whether the alum addition augmented the protection and the effective period of SARS-CoV virion vaccination should be addressed, because currently used inactivated influenza virus whole virion vaccine is significantly effective without any adjuvant. Meanwhile, we also need to develop a potent adjuvant for induction of a much stronger mucosal immunity, in addition to evaluating available methods of virion inactivation.

Acknowledgements

We thank Ms R. Ishida, Ms Y. Kaburagi and Mr Y. Kimishima for their excellent technical help. This work was supported by a grant from the Ministry of Public Health and Labor of Japan.

Abbreviations

ACE2	angiotensin-converting enzyme 2
ASC	antibody-secreting cell
E	envelope
M	membrane
N	nucleocapsid protein
SARS	severe acute respiratory syndrome
SARS-CoV	SARS-associated coronavirus
S	spike protein

References

1 Drosten, C., Gunther, S., Preiser, W. *et al.* 2003. Identification of a novel coronavirus in patients with severe acute respiratory syndrome. *N. Engl. J. Med.* 348:1967.
2 Ksiazek, T. G., Erdman, D., Goldsmith, C. S. *et al.* 2003. A novel coronavirus associated with severe acute respiratory syndrome. *N. Engl. J. Med.* 348:1953.
3 Marra, M. A., Jones, S. J., Astell, C. R. *et al.* 2003. The genome sequence of the SARS-associated coronavirus. *Science* 300:1399.
4 Rota, P. A., Oberste, M. S., Monroe, S. S. *et al.* 2003. Characterization of a novel coronavirus associated with severe acute respiratory syndrome. *Science* 300:1394.
5 Holmes, K. V. and Enjuanes, L. 2003. Virology. The SARS coronavirus: a postgenomic era. *Science* 300:1377.
6 Liu, X., Shi, Y., Li, P., Li, L., Yi, Y., Ma, Q. and Cao, C. 2004. Profile of antibodies to the nucleocapsid protein of the severe acute respiratory syndrome (SARS)-associated coronavirus in probable SARS patients. *Clin. Diagn. Lab. Immunol.* 11:227.
7 De Groot, A. S. 2003. How the SARS vaccine effort can learn from HIV—speeding towards the future, learning from the past. *Vaccine* 21:4095.
8 Li, W., Moore, M. J., Vasilieva, N. *et al.* 2003. Angiotensin-converting enzyme 2 is a functional receptor for the SARS coronavirus. *Nature* 426:450.
9 Collins, R. A., Knobler, R. L., Powell, H. and Buchmeier, M. J. 1982. Monoclonal antibodies to murine hepatitis virus-4 (strain JHM) define the viral glycoprotein responsible for attachment and cell–cell fusion. *Virology* 119:358.
10 Fleming, J. O., Stohlman, S. A., Harmon, R. C., Lai, M. M., Frelinger, J. A. and Weiner, L. P.1983. Antigenic relationship of murine coronaviruses: analysis using monoclonal antibodies to JHM (MHV-4) virus. *Virology* 131:296.
11 Jackwood, M. W. and Hilt, D. A. 1995. Production and immunogenicity of multiple antigenic peptide (MAP) constructs derived from the S1 glycoprotein of infectious bronchitis virus (IBV). *Adv. Exp. Med. Biol.* 380:213.
12 Anton, I. M., Gonzalez, S., Bullido, M. J., Corsin, M., Risco, C., Langeveld, J. P. and Enjuanes, L. 1996. Cooperation between transmissible gastroenteritis coronavirus (TGEV) structural proteins in the *in vitro* induction of virus-specific antibodies. *Virus Res.* 46:111.
13 Ishii, K., Ueda, Y., Matsuo, K. *et al.* 2002. Structural analysis of vaccinia virus DIs strain: application as a new replication-deficient viral vector. *Virology* 302:433.
14 Storch, G. A. 2001. Diagnostic virology. In Knipe, D. M., Howley, P. M., ed., *Fields Virology*, 4th edn. Lippincott Williams & Wilkins, Philadelphia, PA. pp. 493–531.
15 Benner, R., Hijmans, W. and Haaijman, J. J. 1981. The bone marrow: the major source of serum immunoglobulins, but still a neglected site of antibody formation. *Clin. Exp. Immunol.* 46:1.
16 Slifka, M. K., Matloubian, M. and Ahmed, R. 1995. Bone marrow is a major site of long-term antibody production after acute viral infection. *J. Virol.* 69:1895.
17 Schmidt, O. W. and Kenny, G. E. 1982. Polypeptides and functions of antigens from human coronaviruses 229E and OC43. *Infect. Immun.* 35:515.

18 Xiao, X., Chakraborti, S., Dimitrov, A. S., Gramatikoff, K. and Dimitrov, D. S. 2003. The SARS-CoV S glycoprotein: expression and functional characterization. *Biochem. Biophys. Res. Commun.* 312:1159.
19 Singh, M. and O'Hagan, D. 1999. Advances in vaccine adjuvants. *Nat. Biotechnol.* 17:1075.
20 Clements, C. J. and Griffiths, E. 2002. The global impact of vaccines containing aluminium adjuvants. *Vaccine* 20 (Suppl. 3): S24.
21 HogenEsch, H. 2002. Mechanisms of stimulation of the immune response by aluminum adjuvants. *Vaccine* 20 (Suppl. 3): S34.
22 Jordan, M. B., Mills, D. M., Kappler, J., Marrack, P. and Cambier, J. C. 2004. Promotion of B cell immune responses via an alum-induced myeloid cell population. *Science* 304:1808.
23 Weiss, R. C. and Scott, F. W. 1981. Antibody-mediated enhancement of disease in feline infectious peritonitis: comparisons with dengue hemorrhagic fever. *Comp. Immunol. Microbiol. Infect. Dis.* 4:175.
24 Wu, G. F., Dandekar, A. A., Pewe, L. and Perlman, S. 2001. The role of CD4 and CD8 T cells in MHV-JHM-induced demyelination. *Adv. Exp. Med. Biol.* 494:341.
25 Pope, M., Chung, S. W., Mosmann, T., Leibowitz, J. L., Gorczynski, R. M. and Levy, G. A. 1996. Resistance of naive mice to murine hepatitis virus strain 3 requires development of a Th1, but not a Th2, response, whereas pre-existing antibody partially protects against primary infection. *J. Immunol.* 156:3342.
26 Yang, Z. Y., Kong, W. P., Huang, Y., Roberts, A., Murphy, B. R., Subbarao, K. and Nabel, G. J. 2004. A DNA vaccine induces SARS coronavirus neutralization and protective immunity in mice. *Nature* 428:561.
27 Mazumdar, T., Anam, K. and Ali N. 2004. A mixed Th1/Th2 response elicited by a liposomal formation of *Leishmania* vaccine instructs Th1 responses and resistance to *Leishmania donovani* in susceptible BALB/c mice. *Vaccine* 22:1162.
28 Nicollier-Jamot, B., Ogier, A., Piroth, L., Pothier, P. and Kohli, E. 2004. Recombinant virus-like particles of a norovirus (genogroup II strain) administered intranasally and orally with mucosal adjuvants LT and LT(R192G) in BALB/c mice induce specific humoral and cellular Th1/Th2-like immune responses. *Vaccine* 22:1079.
29 Gao, W., Tamin, A., Soloff, A., D'Aiuto, L., Nwanegbo, E., Robbins, P. D., Bellini, W. J., Barratt-Boyes, S. and Gambotto, A. 2003. Effects of a SARS-associated coronavirus vaccine in monkeys. *Lancet 362:1895.*
30 Takamura, K., Matsumoto, Y. and Shimizu, Y. 2002. Field study of bovine coronavirus vaccine enriched with hemagglutinating antigen for winter dysentery in dairy cows. *Can. J. Vet. Res.* 66:278.
31 Pratelli, A., Tinelli, A., Decaro, N., Cirone, F., Elia, G., Roperto, S., Tempesta, M. and Buonavoglia, C. 2003. Efficacy of an inactivated canine coronavirus vaccine in pups. *New Microbiol.* 26:151.

Available online at www.sciencedirect.com

SCIENCE DIRECT

Virology 327 (2004) 169–174

VIROLOGY

www.elsevier.com/locate/yviro

Rapid Communication

Importance of Akt signaling pathway for apoptosis in SARS-CoV-infected Vero E6 cells

Tetsuya Mizutani*, Shuetsu Fukushi, Masayuki Saijo, Ichiro Kurane, Shigeru Morikawa

Special Pathogens Laboratory, Department of Virology 1, National Institute of Infectious Diseases, Musashimurayama, Tokyo 208-0011, Japan

Received 26 May 2004; accepted 9 July 2004

Abstract

Severe acute respiratory syndrome (SARS) is an acute respiratory tract infectious disease that is associated with a new coronavirus (SARS-CoV). Our recent study indicated that SARS-CoV infection induces activation of the p38 mitogen-activated protein kinase (MAPK) signaling pathway and the p38 MAPK inhibitor partially inhibited its cytopathic effect in Vero E6 cells. The results of the present study indicated that before cell death, Akt, which is an inhibitor of apoptosis, was also activated in response to viral replication. Phosphorylation of a serine residue on Akt was detected at least 8 h postinfection (hpi), which declined after 18 hpi. Thus, the phosphatidylinositol 3-kinase (PI3K)/Akt pathway is activated in virus-infected Vero E6 cells. However, a threonine residue was not phosphorylated. A downstream target of Akt, glycogen synthase kinase 3β (GSK-3β), was slightly phosphorylated, indicating that the level of activation of Akt was very low. PKCζ, which is downstream of the PI3K pathway, was also phosphorylated in virus-infected cells. These results suggested that weak activation of Akt cannot prevent apoptosis induced by SARS-CoV infection in Vero E6 cells.

Keywords: SARS-CoV; Akt; PI3K; PKC

Severe acute respiratory syndrome (SARS) is a newly described infectious disease caused by a coronavirus (Rota et al., 2003). Although the mechanism of SARS pathogenesis in vivo may involve both the effect of viral replication in target cells and immune responses, there is a lack of molecular pathological data including signaling pathways of SARS-coronavirus (CoV) infection. Recently, we reported that infection with SARS-CoV caused apoptosis in Vero E6 cells and that p38 mitogen-activated protein kinase (MAPK) was activated during infection (Mizutani et al., 2004). Thus, it is important to investigate the apoptotic events that occur in SARS-CoV-infected cells to understand the pathogenesis of SARS-CoV. Generally, both pro-apoptotic and pro-survival signaling pathways are activated after apoptotic signaling, and there are many pro- and anti-apoptotic proteins involved in these pathways in cells. The present study was performed to clarify the activated signaling pathways related to apoptotic events in SARS-CoV-infected Vero E6 cells.

In SARS-CoV-infected Vero E6 cells, cytopathic effects were observed within 24 h postinfection (hpi). We have recently shown that p38 MAPK and its downstream targets are phosphorylated in SARS-CoV-infected Vero E6 cells (Mizutani et al., 2004). These findings suggest that other signaling pathways are also activated in SARS-CoV-infected cells. To investigate such cellular responses in SARS-CoV-infected Vero E6 cells before apoptosis, proteins of SARS-CoV-infected and mock-infected cells were analyzed by Western blotting analysis at 18 hpi using 125 antibodies to human cellular proteins. We found that antibodies to proteins related to several signaling pathways responded specifically in SARS-CoV infection (\ below and unpublished data).

One such signaling pathway, protein kinase B (PKB), known as Akt, has been studied intensively (Toker, 2000;

* Corresponding author. Special Pathogens Laboratory, Department of Virology 1, National Institute of Infectious Diseases, Gakuen 4-7-1, Musashimurayama, Tokyo 208-0011, Japan. Fax: +81 42 564 4881.
E-mail address: tmizutan@nih.go.jp (T. Mizutani).

0042-6822/$ - see front matter © 2004 Elsevier Inc. All rights reserved.
doi:10.1016/j.virol.2004.07.005

Brazil and Hemmings, 2001; Scheid and Woodgett, 2003). Akt is phosphorylated at both serine 473 and threonine 308 residues through a phosphatidylinositol 3-kinase (PI3K)-dependent mechanism on stimulation by growth factors, insulin, and hormones (Welch et al., 1998). An important function of activated Akt in cells is inhibition of apoptosis. Downstream targets of Akt induce cell survival via phosphorylation of the forkhead transcription factor (FKHR) family, glycogen synthase kinase 3β (GSK-3β), caspase-9, and Bad (Cardone et al., 1998; Cross et al., 1995; Datta et al., 1997). To examine the phosphorylation of Akt in virus-infected cells, Western blotting analysis was performed using anti-phospho Akt antibodies. As shown in Fig. 1A, serine 473 of Akt was phosphorylated at 8 hpi by SARS-CoV. The phosphorylated serine 473 of Akt began to accumulate at least 8 hpi and maximal phosphorylation was observed at 18 hpi. Western blotting analysis with a phosphorylation-state-independent anti-Akt antibody revealed the presence of Akt in Vero E6 cells, whereas a threonine 308 phosphorylation-state-dependent antibody failed to demonstrate the presence of threonine 308 phosphorylated Akt in virus-infected cells (Fig. 1A). In addition, serine phosphorylation was dependent on SARS-CoV infection into Vero E6 cells, because the UV-inactivated virus failed to induce serine phosphorylation. Brief stimulation by epidermal growth factor (EGF) also showed only serine 473 phosphorylation of Akt (Fig. 1B), suggesting that threonine 308 of Akt is difficult to phosphorylate in Vero E6 cells. Therefore, total activity of Akt may be low in Vero E6 cells. However, it is possible that the anti-phospho Akt (threonine 308) antibody used in the present study is unable to recognize threonine phosphorylation of Akt in Vero E6 cells as the datasheet included no description of cross-reactivity with monkey. To investigate whether SARS-CoV-induced Akt serine phosphorylation represented a biologically active kinase, we examined the in vitro kinase activity of phosphorylated Akt in SARS-CoV-infected cells. The SARS-CoV-infected Vero E6 cells were lysed at 18 hpi and serine 473-phosphorylated Akt in the cell lysate was precipitated by anti-serine 473-phosphorylated Akt antibody. GSK-3β protein was added to the immunoprecipitated phosphorylated Akt with ATP, and Western blotting was performed using anti-phosphorylated GSK-3α/β (Ser21/9) antibody. As shown in Fig. 1C, immunoprecipitated Akt was almost at the same amount between SARS-CoV-infected cells and mock-infected cells at 18 hpi. The amount of serine 473-phosphorylated Akt in SARS-CoV-infected cells was higher than that in mock-infected controls. The level of phosphorylation of GSK-3α/β in virus-infected cells was slightly higher than that in mock-infected controls. These results strongly suggested that Akt in Vero E6 cells was phosphorylated only at serine residues by SARS-CoV infection, but the level of activity of Akt was low.

To investigate phosphorylation of up- and downstream targets of Akt in virus-infected cells, Western blotting analysis was performed. Of the Akt targets mentioned above, the level of phosphorylation of GSK-3β (Ser9) was slightly increased, while phosphorylated Bad and FKHR were not detected (Fig. 1C). GSK-3 β is a pro-apoptotic signaling molecule and is inactivated by phosphorylation of the N-terminal serine residue Ser9 (Pap and Cooper, 1998).

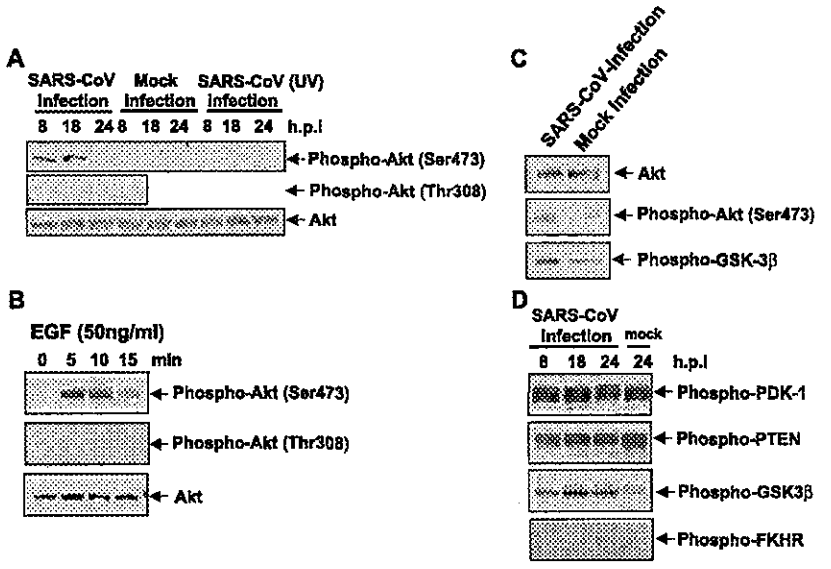

Fig. 1. Phosphorylation of Akt in SARS-CoV-infected Vero E6 cells. (A) Vero E6 cells were infected with SARS-CoV at moi of 5, and Western blotting was then performed using proteins obtained at 8, 18, and 24 hpi. FCS-free medium and UV-inactivated SARS-CoV were used as controls. Phosphorylated Akt was detected by Western blotting analysis. (B) EGF was added to Vero E6 cells for 5, 10, and 15 min. (C) In vitro Akt kinase assay was performed using proteins from SARS-CoV-infected Vero E6 cells and mock-infected cells at 18 hpi. (D) Phosphorylation of up- and downstream targets of Akt was detected by Western blotting analysis.

Therefore, these results suggested that the phosphorylation of Akt in Vero E6 cells results in a low level of anti-apoptotic response to SARS-CoV infection. Recent studies explained the activation cycle of Akt as outlined below (Toker, 2000; Brazil and Hemmings, 2001; Scheid and Woodgett, 2003). Activation of PI3K results in local accumulation of phosphatidylinositol (PtdIns)-3,4,5-triphosphate (P3) at the plasma membrane, and PTEN phosphatase inhibits PI3K signaling. Cytosolic Akt is inactive and the activity of cytosolic PDK-1 is low. PtdIns-3,4,5-P3 recruits PDK-1 and Akt to the plasma membrane, and then Akt is autophosphorylated at serine 473. After PDK-1 activation on the plasma membrane, PDK-1 phosphorylates Akt on threonine 308, and then Akt shows a high level of activity. Thus, activation of upstream kinases of Akt is important for the activation of Akt. Fig. 1C shows that the amounts of both phosphorylated PTEN and PDK-1 were not significantly altered in SARS-CoV-infected Vero E6 cells. Therefore, these results may explain why no increase in threonine 308 phosphorylation of Akt was observed on virus infection.

The PI3 kinase inhibitor LY294002 is widely used to study Akt phosphorylation in stimulations in vitro. We examined whether LY294002 inhibits serine phosphorylation of Akt induced by SARS-CoV infection. Vero E6 cells were treated with LY294002 (10 and 20 μM) for 1.5 h, and then infected with SARS-CoV. Western blotting analysis was performed on the cell lysate at 18 hpi. As shown in Fig. 2A, the serine residue of Akt was not phosphorylated in cells treated with either concentration of LY294002. This result suggested that serine phosphorylation of Akt was sensitive to the PI3K inhibitor and that PI3K was activated in virus-infected cells. In addition, DNA fragmentations in infected Vero E6 cells at 30 hpi were similar in the presence and absence of LY294002 (Fig. 2B), suggesting that weak activation of Akt cannot prevent apoptosis induced by SARS-CoV infection in Vero E6 cells.

As shown in Fig. 2A, the level of viral N protein expression seemed to be similar at 18 hpi among cells treated with various amounts of LY294002. Next, we investigated whether enhancement of virus-specific protein synthesis through Akt-serine 473 phosphorylation occurs in SARS-CoV-infected cells at early time points pi. Recently, Simmons et al. (2004) reported that acidification of endosomes was required for SARS-CoV S-mediated viral entry using S glycoprotein pseudoviruses, after viral adsorption to angiotensin-converting enzyme (ACE)2 (Li et al., 2003). They reported that SARS-CoV S protein is cleaved in the presence of trypsin and that the cleaved S induces cell fusion. Their results suggested that SARS-CoV enters cells via endocytosis. Before a virus infection experiment, to verify that LY294002 has no effect on acidification of intracellular compartments in Vero E6 cells, LY294002 was added to the cells, followed by staining with acridine orange to detect intracellular acidic compartments (Mizutani et al., 2003). As indicated in Fig. 2C, neither 10 nor 20 μM LY294002 had any effect on the acidification of intracellular compartments, suggesting that treatment with LY294002 did not inhibit endocytosis in Vero E6 cells. Next, Western blotting analysis was performed at 6, 9, and 12 hpi using anti-N antibody. As shown in Fig. 2D, the kinetics of SARS-CoV-N protein accumulation in infected Vero E6 cells were similar in the presence and absence of LY294002. These

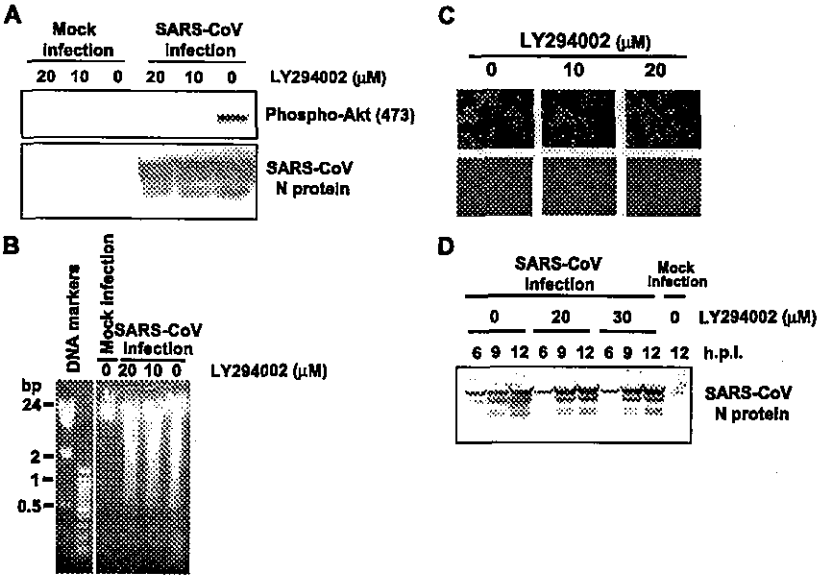

Fig. 2. Effects of LY294002 on SARS-CoV infection. (A) Vero E6 cells were pretreated with LY294002 and then infected with SARS-CoV at moi of 5. Western blotting analysis was performed at 18 hpi. (B) Cellular DNA was extracted from Vero E6 cells in the presence or absence of LY294002 at 30 hpi. (C) Vero E6 cells were incubated for 1.5 h with LY294002 and stained with acridine orange. (D) Western blotting analysis was performed at 6, 9, and 12 hpi for detection of SARS-CoV N protein.

results indicated that Akt serine phosphorylation induced by SARS-CoV infection had no effect on viral replication.

Protein kinase C (PKC) is also a major cellular mediator of biological functions. The PKC superfamily is divided into sub-superfamilies according to their activation profiles; conventional PKC (cPKC α, βI, βII, γ novel PKC (nPKC δ, ε, η, θ), atypical PKC (aPKCζ, ι/λ), PKCμ/PKD, and PKCυ (Toker, 2000). PKCζ was originally discovered as a unique PKC isotype (Ono et al., 1989). B cell survival by nerve growth factor (NGF) is mediated by PI3K-dependent activation of PKCζ (Kronfeld et al., 2002) and Akt could interact with PKCζ (Konishi et al., 1994). To determine if PKCζ is phosphorylated by SARS-CoV infection, Western blotting analysis was performed using an anti-phospho PKCζ (Thr410) antibody. As shown in Fig. 3, PKCζ was phosphorylated at 8 hpi, suggesting that PKCζ is activated as an anti-apoptotic response to virus infection. The antibody used in the present study can also detect phosphorylated PKCλ, and the function of PKCζ is still not clear. A novel PKC subfamily PKCθ was also very slightly phosphorylated by virus infection. In addition, PKCα/βII and δ (Ser643) were always phosphorylated in both virus-infected and mock-infected cells. These results suggested that the interaction of phosphorylation of PKCζ with Akt plays an important role in protection against SARS-CoV infection (Fig. 4).

In the present study, we showed that the PI3K/Akt pathway including PKCζ is activated by SARS-CoV infection, but that the level of activation of Akt in infected cells is very low. In virus infection, two conflicting cellular programs are triggered in cells: apoptosis to eliminate virus-infected cells and cell survival delaying cell death to alert naive cells by producing antiviral cytokines. This raises the question of how cell survival or death of SARS-CoV-infected cells is determined. The control mechanisms that balance cell survival against cell death are not well understood.

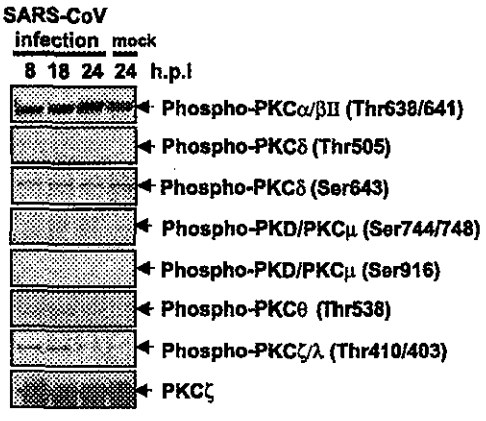

Fig. 3. Phosphorylation of PKCs in SARS-CoV-infected Vero E6 cells. Phosphorylated PKCs were detected by Western blotting analysis using proteins isolated from SARS-CoV-infected Vero E6 cells at 8, 18, and 24 hpi.

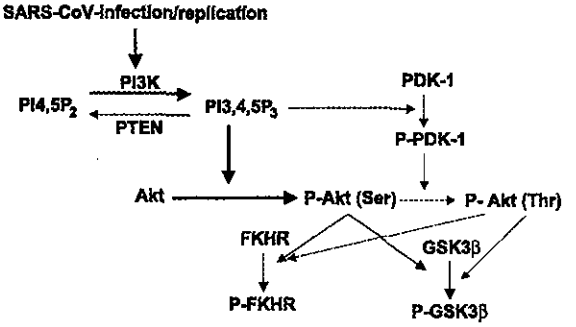

Fig. 4. Phosphorylation of Akt/PI3K signaling pathway in SARS-CoV-infected Vero E6 cells. Bold lines indicate activated pathways in viral-infected cells. Week or no activated pathways are indicated by thin lines.

Previously, we showed that activation of the p38 MAPK signaling pathway induced by SARS-CoV infection has a partially pro-apoptotic role in Vero E6 cells (Mizutani et al., 2004). The role of p38 MAPK signaling in cellular responses is diverse depending on the cell type and stimulus. For example, p38 MAPK signaling has been shown to promote cell death as well as to enhance cell growth and survival (Juretic et al., 2001; Liu et al., 2001; Yosimichi et al., 2001). In virus-infected Vero E6 cells, CREB and HSP-27, which have anti-apoptotic roles, were shown to be phosphorylated (Mizutani et al., 2004). Therefore, pro-apoptotic molecules downstream of targets of p38 MAPK may exist in Vero E6 cells. On the other hand, Akt, which is a key regulator of cell survival events, targets several different cytoplasmic proteins, including pro-apoptotic molecules, such as GSK3β, caspase-9, Bad, and FKHR. Phosphorylation of these proteins by Akt generally results in their inactivation and inability to activate pro-apoptotic pathways. In the present study, phosphorylation of GSK3β serine 9 was found in virus-infected cells. However, our results suggested that the level of phosphorylation of GSK3β is not sufficient to prevent apoptosis.

In conclusion, incomplete activation of Akt induces apoptosis in SARS-CoV-infected Vero E6 cells. However, we cannot exclude the possibility of the involvement of other signaling pathways that strongly induce apoptosis. These findings may facilitate the development of a new way to block apoptosis upstream and help in the development of anti-SARS-CoV agents.

Materials and methods

Cells and virus

Vero E6 cells were routinely subcultured in 75-cm^3 flasks in Dulbecco's modified Eagle's medium (DMEM, Sigma, St. Louis, MO, USA) supplemented with 0.2 mM L-glutamine, 100 units/ml penicillin, 100 μg/ml streptomycin, and 5% (v/v) fetal bovine serum (FBS), and maintained at

37 °C in an atmosphere of 5% CO_2. For use in the experiments, the cells were split once they reached 90% confluence and seeded onto 6- or 24-well tissue culture plate inserts. The culture medium was changed to 2% FBS containing DMEM before virus infection. In the present study, we used SARS-CoV (Drosten et al., 2003), which was isolated as Frankfurt 1 (Thiel et al., 2003) and kindly provided by Dr. J. Ziebuhr. Infection was usually performed with a multiplicity of infection (moi) of 5.

Western blotting

After virus infection, whole-cell extracts were electrophoresed in 12.5% and 10–20% gradient polyacrylamide gels, and transferred onto PVDF membranes (Immobilon-P, Millipore, Bedford, MA, USA). We applied two sets of samples to polyacrylamide gels, and the blots were divided into two sheets. The following antibodies were used at a dilution of 1:1000 (Cell Signaling Technology Inc., Beverly, MA, USA): Rabbit anti-phospho Akt (Ser473), rabbit anti-phospho Akt (Thr308), rabbit anti-Akt, rabbit anti-phospho GSK-3β (Ser9), anti-phospho FKHR (Ser256), anti-phospho PTEN (Ser380), rabbit anti-phospho PDK-1, rabbit Phospho-PKCα/βII (Thr638/641) antibody, rabbit anti-phospho-PKCδ (Thr505) antibody, rabbit anti-phospho-PKCδ (Ser643) antibody, rabbit anti-phospho-PKD/PKCμ (Ser744/748) antibody, rabbit anti-phospho-PKD/PKCμ (Ser916) antibody, rabbit anti-phospho-PKCζ (Thr538) antibody, and rabbit anti-phospho-PKCζ/λ (Thr410/403) antibody. Rabbit anti-PKCζ antibody (diluted 1:1000) was purchased from Santa Cruz Biotechnology (Santa Cruz, CA, USA). Rabbit anti-SARS N and M antibodies were described previously (Mizutani, 2004). After 15-h incubation, the membrane was washed with 0.1% TBS-Tween and specific proteins were detected with a ProtoBlot II AP system (Promega Co., Madison, WI, USA), as described previously (Mizutani et al., 2003).

In vitro GSK-3 activation assay

Vero E6 cells were infected with SARS-CoV at moi of 10 for 18 hpi, and then cell extracts were obtained using the lysis buffer supplied with the Akt kinase assay kit (Cell Signaling Technology Inc., Bedford, MA, USA). Selective immunoprecipitation of Akt was performed using immobilized Akt (serine phosphorylation) antibody. After incubation of immunoprecipitated Akt in kinase buffer containing GSK-3β fusion protein and ATP, GSK-3α/β (Ser21/9) phosphorylation was analyzed by Western blotting using anti-phospho GSK-3 antibody.

DNA fragmentation

Vero E6 cells were pretreated with LY294002 for 1.5 h, and then 5 moi of SARS-CoV was inoculated. At 30 hpi, DNA was extracted using MEBCYTO Apoptosis ladder detection kit (Medical and Biological Laboratories, Co. LTD., Nagoya, Japan), as described previously (Mizutani et al., 2004). The DNA was analyzed by electrophoresis on 1% agarose gels and then stained with ethidium bromide.

Endocytosis assay

Vero E6 cells at 50% confluency in 24-well plates were incubated for 1.5 h with 10 or 20 μM LY294002 (Cell Signaling Technology Inc.) or dimethyl sulfoxide (DMSO) in 1 ml of medium. The LY294002 was dissolved in DMSO. The medium was removed and 5 μg/ml of acridine orange (Wako, Osaka, Japan) in Mg^{2+}-free Hank's solution was added to the cells. After incubation for 5 min, the cells were washed twice with Hank's solution, followed by addition of 0.5% trypan blue solution. Fluorescence micrographs were taken at the same shutter speed for each experiment.

Acknowledgments

We thank Dr. F. Taguchi (National Institute of Infectious Diseases, Japan) for useful suggestions. We also thank Ms. M. Ogata (National Institute of Infectious Diseases, Japan) for her assistance. This work was supported in part by a grant-in-aid from the Ministry of Health, Labor, and Welfare of Japan and the Japan Health Science Foundation, Tokyo, Japan.

References

Brazil, D.P., Hemmings, B.A., 2001. Ten years of protein kinase B signalling: a hard Akt to follow. Trends Biochem. Sci. 26, 657–664.

Cardone, M.H., Roy, N., Stennicke, H.R., Salvesen, G.S., Franke, T.F., Stanbridge, E., Frisch, S., Reed, J.C., 1998. Regulation of cell death protease caspase-9 by phosphorylation. Science 282, 1318–1321.

Cross, D.A., Alessi, D.R., Cohen, P., Andjelkovich, M., Hemmings, B.A., 1995. Inhibition of glycogen synthase kinase-3 by insulin mediated by protein kinase B. Nature 378, 785–789.

Datta, S.R., Dudek, H., Tao, X., Masters, S., Fu, H., Gotoh, Y., Greenberg, M.E., 1997. Akt phosphorylation of BAD couples survival signals to the cell-intrinsic death machinery. Cell 91, 231–241.

Drosten, C., Gunther, S., Preiser, W., et al., 2003. Identification of a novel coronavirus in patients with severe acute respiratory syndrome. N. Engl. J. Med. 348, 1967–1976.

Juretic, N., Santibanez, J.F., Hurtado, C., Martinez, J., 2001. ERK 1,2 and p38 pathways are involved in the proliferative stimuli mediated by urokinase in osteoblastic SaOS-2 cell line. J. Cell. Biochem. 83, 92–98.

Konishi, H., Shinomura, T., Kuroda, S., Ono, Y., Kikkawa, U., 1994. Molecular cloning of rat RAC protein kinase alpha and beta and their association with protein kinase C zeta. Biochem. Biophys. Res. Commun. 205, 817–825.

Kronfeld, I., Kazimirsky, G., Gelfand, E.W., Brodie, C., 2002. NGF rescues human B lymphocytes from anti-IgM induced apoptosis by activation of PKC. Eur. J. Immunol. 32, 136–143.

Li, W., Moore, M.J., Vasilieva, N., Sui, J., Wong, S.K., Berne, M.A., Somasundaran, M., Sullivan, J.L., Luzuriaga, K., Greenough, T.C., Choe, H., Farzan, M., 2003. Angiotensin-converting enzyme 2 is a functional receptor for the SARS coronavirus. Nature 426, 450–454.

Liu, B., Fang, M., Lu, Y., Lu, Y., Mills, G.B., Fan, Z., 2001. Involvement of JNK-mediated pathway in EGF-mediated protection against paclitaxel-induced apoptosis in SiHa human cervical cancer cells. Br. J. Cancer. 85, 303–311.

Mizutani, T., Kobayashi, M., Eshita, Y., Shirato, K., Kimura, T., Ako, Y., Miyoshi, H., Takasaki, T., Kurane, T., Kariwa, H., Umemura, T., Takashima, I., 2003. Involvement of the *JNK-like protein* of the Aedes albopictus mosquito cell line, C6/36, in phagocytosis, endocytosis and infection of West Nile virus. Insect. Mol. Biol. 12, 491–499.

Mizutani, T., Fukushi, S., Morikawa, S., Saijo, M., Kurane, I., 2004. Phosphorylation of p38 MAPK and its downstream targets in SARS coronavirus-infected cells. Biochem. Biophys. Res. Commun. 319, 1228–1234.

Ono, Y., Fujii, T., Ogita, K., Kikkawa, U., Igarashi, K., Nishizuka, Y., 1989. Protein kinase C-subspecies from brain: its structure, expression and properties. Proc. Natl. Acad. Sci. U.S.A. 86, 3099–3103.

Pap, M., Cooper, G.M., 1998. Role of glycogen synthase *kinase-3* in the phosphatidylinositol 3-Kinase/Akt cell survival pathway. J. Biol. Chem. 273, 19929–19932.

Rota, P.A., Oberste, M.S., Monroe, S.S., et al., 2003. Characterization of a novel coronavirus associated with severe acute respiratory syndrome. Science 300, 1394–1399.

Scheid, M.P., Woodgett, J.R., 2003. Unravelling the activation mechanisms of protein kinase B/Akt. FEBS Lett. 546, 108–112.

Simmons, G., Reeves, J.D., Rennekamp, A.J., Amberg, S.M., Piefer, A.J., Bates, P., 2004. Characterization of severe acute respiratory syndrome-associated coronavirus (SARS-CoV) spike glycoprotein-mediated viral entry. Proc. Natl. Acad. Sci. U.S.A. 101, 4240–4245.

Thiel, V., Ivanov, K.A., Putics, A., Hertzig, T., Schelle, B., Bayer, S., Weissbrich, B., Snijder, E.J., Rabenau, H., Doerr, H.W., Gorbalenya, A.E., Ziebuhr, J., 2003. Mechanisms and enzymes involved in SARS coronavirus genome expression. J. Gen. Virol. 84, 2305–2315.

Toker, A., 2000. Protein kinases as mediators of phosphoinositide 3-kinase signaling. Mol. Pharmacol. 57, 652–658.

Welch, H., Eguinoa, A., Stephens, L.R., Hawkins, P.T., 1998. Protein kinase B and rac are activated in parallel within a phosphatidylinositide 3OH-kinase-controlled signaling pathway. J. Biol. Chem. 273, 11248–11256.

Yosimichi, G., Nakanishi, T., Nishida, T., Hattori, T., Takano-Yamamoto, T., Takigawa, M., 2001. CTGF/Hcs24 induces chondrocyte differentiation through a p38 mitogen-activated protein kinase (p38MAPK), and proliferation through a p44/42 MAPK/extracellular-signal regulated kinase (ERK). Eur. J. Biochem. 268, 6058–6065.

Available online at www.sciencedirect.com
SCIENCE DIRECT
Virus Research 98 (2003) 83–91
Virus Research
www.elsevier.com/locate/virusres

Association of the nucleocapsid protein of the Seoul and Hantaan hantaviruses with small ubiquitin-like modifier-1-related molecules

Byoung-Hee Lee[a], Kumiko Yoshimatsu[a], Akihiko Maeda[b], Kazuhiko Ochiai[c], Masami Morimatsu[c], Koichi Araki[d], Michiko Ogino[a], Shigeru Morikawa[b], Jiro Arikawa[a,*]

[a] *Institute for Animal Experimentation, Graduate School of Medicine, Hokkaido University, Kita-15, Nishi-7, Kita-ku, Sapporo 060-8638, Japan*
[b] *Department of Virology 1, National Institute of Infectious Diseases, Musashimurayama 208-0011, Japan*
[c] *Laboratory of Veterinary Physiology, Faculty of Agriculture, Iwate University, Morioka 020-8550, Japan*
[d] *Laboratory of Public Health, Department of Environmental Veterinary Science, Graduate School of Veterinary Medicine, Hokkaido University, Sapporo 060-0818, Japan*

Received 17 June 2003; received in revised form 28 August 2003; accepted 2 September 2003

Abstract

We performed yeast two-hybrid screening of a human kidney cell cDNA library to study the biological role of the hantavirus nucleocapsid protein (NP). We found that Seoul virus (SEOV) and Hantaan virus (HTNV) NPs were associated with small ubiquitin-like modifier (SUMO)-1-interacting proteins PIAS1, PIASxβ, HIPK2, CHD3, and TTRAP, which interacted with the SUMO-1 conjugating enzyme (Ubc-9) and SUMO-1 in the yeast two-hybrid assay. Interactions between the HIPK2, CHD3, and TTRAP proteins and SEOV NP were also shown in a mammalian two-hybrid assay. However, there was no interaction between PIAS proteins and NP, which was probably due to the inhibitory effect of PIAS on transcription in the mammalian two-hybrid assay. Nevertheless, a co-expression experiment suggested the existence of a PIAS-NP interaction in the cytoplasm. The region spanning amino acids 100–125 of SEOV NP, which represents a critical region for NP–NP polymerization, was found to be responsible for the interaction with SUMO-1-related molecules in both the yeast and mammalian two-hybrid assays. These results add to the information on interactions of hantavirus NP and host cellular proteins.

Keywords: Hantavirus; SUMO-1; NP; PIAS; Ubc9; HFRS; Two-hybrid assay

1. Introduction

Hantaviruses are tripartite negative-sense RNA viruses in the *Hantavirus* genus of the Bunyaviridae family (Schmaljohn and Dalrymple, 1983). They are the etiologic agents of two distinct diseases in humans, hemorrhagic fever with renal syndrome and hantavirus pulmonary syndrome, which are transmitted from rodents to humans (Schmaljohn and Hjelle, 1997).

The hantaviral genome contains large (L), medium (M), and small (S) viral RNA segments that encode the RNA-dependent RNA polymerase (L protein), two surface glycoproteins (G1 and G2), and the nucleocapsid protein (NP), respectively. NP is antigenically and genetically more conserved than the envelope proteins among the various hantaviruses (Elliott, 1990). In general, NP plays an important role in intracellular events, such as replication and transcription. For example, the vesicular stomatitis virus (VSV) NP modulates the transition from transcription to replication (Patton et al., 1984), and the influenza virus NP is required for RNA synthesis (Nakagawa et al., 1995). Selective encapsidation of viral genomic or leader RNAs has been reported for the VSV and rabies viruses (Patton et al., 1984; Yang et al., 1999). Although little is known about the mechanism of viral RNA encapsidation in hantaviruses, NP clearly functions in the viral replication cycle through its interactions with the viral nucleic acids, other viral structural proteins, and host cell proteins (Severson et al., 1999).

One type of virus–host interaction that is well established and widespread is the functional modulation of viral proteins by post-translational modifications, such as phosphorylation, glycosylation, and ubiquitinylation. More

* Corresponding author. Tel.: +81-11-706-6905; fax: +81-11-706-7879.
E-mail address: j_arika@med.hokudai.ac.jp (J. Arikawa).

0168-1702/$ – see front matter © 2003 Elsevier B.V. All rights reserved.
doi:10.1016/j.virusres.2003.09.001

recently, a novel post-translational modification, sumoylation has been defined which involves the conjugation of a small ubiquitin-like modifier (SUMO-1) to the lysine side chain of a target protein via isopeptide bonding (Saitoh et al., 1997). The conjugation of SUMO-1 to cellular proteins has been implicated in several vital cellular processes, which include nuclear transport, cell cycle control, and oncogenesis (Muller et al., 2001). The effect of sumoylation on viral proteins appears to be substrate-specific, but has functional consequences that are likely to be important for the viral replication cycle (Wilson and Rangasamy, 2001).

Several families of ubiquitin-like proteins have been described, and SUMO-1 is the most prominent of these molecules. As is the case with other ubiquitin conjugation processes, the E1 (activation), E2 (conjugation), and E3 (ligation) enzymes are expected to be involved in the sumoylation process. Previously, the E1 and E2 proteins were reported as Aos1/Uba2 and Ubc9, respectively (Desterro et al., 1997; Gong et al., 1999; Lee et al., 1998). Recently, several studies reported that proteins of the PIAS and *Siz* families had E3-like activities for sumoylation in both mammals and yeasts (Johnson and Gupta, 2001; Kahyo et al., 2001; Takahashi et al., 2001).

Recently, it was reported that the NP of Puumala virus (PUUV), which is a species of hantavirus, interacted with Daxx (a Fas-mediated apoptosis enhancer) (Li et al., 2002), Ubc9, and SUMO-1 (Kaukinen et al., 2003). We elucidated the interactions of both SUMO-1 and the SUMO-1-conjugating enzyme (Ubc9) with the Hantaan virus (HTNV) NP, using yeast and mammalian two-hybrid screens of a HeLa cell cDNA library (Maeda et al., 2003). To obtain further information on the host proteins that interact with the hantavirus NP, we carried out a yeast two-hybrid screening, using a human kidney cell cDNA library. In this report, we show that the NPs of the Seoul virus (SEOV), which is a species of hantavirus, and of HTNV interact not only with the SUMO-1 conjugating enzyme (Ubc9), but also with the ligating enzyme (PIAS) and SUMO-1-related molecules.

2. Materials and methods

2.1. Viruses and cells

Two species of hantavirus, Hantaan virus strain 76118 clone-1 (HTNV) and Seoul virus strain SR-11 (SEOV), were used in this study. The E6 clone of the Vero cell lines (American Type Culture Collection C1008, CRL1586) was grown in the presence of 5% CO_2 air at 37 °C in Eagle's minimal essential medium (MEM; Gibco BRL) that was supplemented with 10% fetal calf serum (FCS), 100 μM MEM non-essential amino acids (Gibco BRL), kanamycin (60 mg/l), streptomycin (100 mg/l), and penicillin (100,000 U/l). The HEK 293 cells and Hela cells (RIKEN cell bank) were maintained in the presence of 5% CO_2 air at 37 °C in Dulbecco's modified Eagle's medium (DMEM; Gibco BRL) that was supplemented with 10% FCS, streptomycin (38 mg/l), and penicillin (50,000 U/l).

2.2. Plasmids for the yeast two-hybrid assay

The yeast-*Escherichia coli* shuttle plasmids that contained the GAL4 DNA-binding domain (pGBT9) and the GAL4-activation domain (pGAD424) were obtained from Clontech (Clontech, Palo Alto, CA). The plasmids pGBT9/SEOV 1–429 (entire NP), pGBT9/SEOV 50–429, pGBT9/SEOV 100–429, pGBT9/SEOV 125–429, pGBT9/SEOV 100–412, and pGBT9/SEOV 1–420 were generated from the cDNA for the SEOV NP (M34881), which was fused in-frame with the GAL4-binding or -activation domains. Plasmid pGBT9/SEOV 100–412 was generated from pGBT9/SEOV 100–429 using the internal *Bgl*II restriction enzyme site. Similarly, plasmid pGBT9/HTNV 1–429 (entire NP) was generated from the cDNA for the NP of HTNV (M14626), which was fused in-frame to the GAL4-binding domain. The GeneEditor in vitro Site-directed Mutagenesis System (Promega, Madison, WI) was used to produce mutant NP that had a tryptophan to alanine alteration at residue 119 (W119A mutation). The Ubc9 and SUMO-1 cDNAs were synthesized by reverse transcription from mRNA that was extracted from HeLa cells. The PCR products were digested with the *Bam*HI restriction enzyme and cloned into the *Bam*HI site of the binding vector pGBT, to clone the sequences in the sense direction (referred to as pGBT/Ubc9 and pGBT/SUMO-1). All of the plasmid constructs were sequenced, to confirm the absence of any mutation in the junctions or inserts. These plasmids were transformed into the yeast two-hybrid assay according to the manufacturer's instructions (Clontech).

2.3. Plasmids for the mammalian cell two-hybrid assay

For the mammalian cell two-hybrid assay, the coding sequences for the SEOV NP and SUMO-1-related molecules were cloned into the pM and pVP plasmids (Clontech). To generate the luciferase reporter plasmid pGluc, the GAL4 promoter from pG5 CAT (Clontech) was cloned into the pGL3-luc vector (Promega), as described previously (Marmorstein et al., 1998). The plasmid DNA was transfected transiently into cells using FuGENE6 (Roche Diagnostics, Mannheim, Germany). Approximately 2×10^5 cells were cotransfected with 50 ng pVP, 50 ng pM, 100 ng pGluc, and 1 ng pRL-TK. The cells were harvested 48 h after transfection, and luciferase activity was measured using the Dual-luciferase Reporter Assay System (Promega). The transfection efficiency was normalized by measuring *Renilla* luciferase activities after cotransfection of the cells with the pRL-TK *Renilla* luciferase plasmid (Promega).

2.4. Two-hybrid screening of cDNA libraries

Human kidney cell cDNA (Matchmaker; Clontech) cloned in the prey plasmid pACT (Clontech) was screened for proteins that interacted with NP, using the yeast reporter strain AH109 (*MATa, trp1-901, leu2-3, 112, ura3-52, his3-200, gal4?, gal80?, LYS2::GAL1$_{UAS}$-GAL1$_{TATA}$-HIS3, GAL2$_{UAS}$-GAL2$_{TATA}$-ADE2, URA3::MEL1$_{UAS}$-MEL1$_{TATA}$-lacZ*) according to the manufacturer's instructions (PT-3183-1; Clontech). The prey and bait plasmids were cotransformed into AH109 using the lithium-acetate method. The transformed cells were plated directly onto minimal medium that lacked adenine, histidine, leucine, and tryptophan, and which was supplemented with 5 mM 3-aminotriazole. Positive clones were isolated, and the permeated cells were retested for β-galactosidase (β-gal) activity. Plasmids from the positive isolates were transformed into *E. coli* strain DH5a, and the plasmid DNA was re-isolated and analyzed by restriction enzyme digestion. Unique inserts were sequenced, and the sequences were compared with those in the databases at the Center for Information Biology and the DNA Data Bank of Japan (Lipman and Pearson, 1985). Each insert was tested systematically in the β-gal assay for interactions with proteins that contained the GAL4-binding domain (BD) fused to full-length and deletion derivatives of NP.

2.5. Antibodies

The monoclonal antibody (MAb) clone ECO2 directed against the SEOV NP was supplied by Dr. C.J. Peters of the Centers for Disease Control and Prevention, Atlanta, GA, USA. The MAb clone E5G6, which is directed against the HTNV NP, was prepared as described previously (Yoshimatsu et al., 1996). The MAbs were purified from mouse ascitic fluids using the Bio-Rad MAPS II kit, which employs a protein A column system. The purified anti-NP MAb was labeled with Alexa Fluor 647, using a monoclonal antibody labeling kit according to the manufacturer's instructions (Molecular Probes, Eugene, OR).

2.6. Localization of NP and PIAS

To analyze the colocalization of NP and PIAS, the expression plasmid for the PIASxβ–GFP fusion protein (Miyauchi et al., 2002; gift from Dr. Hideyo Suzuki), and the expression plasmid vectors containing either the entire or truncated NP were cotransfected into Vero E6 cells. The cDNA clones that contained the coding regions of the S segment of HTNV and SEOV were kindly provided by Dr. C.S. Schmaljohn. The cDNAs of the S segments of HTNV and SEOV were excised, and subcloned into the expression vector pCAGGS/MCS (Niwa et al., 1991). The plasmids that contained the S segment cDNAs of HTNV, SEOV and SEOV NP 125–429 were designated pCHTNS, pCSEOS and pCSEOS125, respectively. Vero E6 cell monolayers (80% confluent) in LabTek chambers (Nalge Nunc, Naperville, IL) were transfected with 50 ng of the expression plasmid for GFP–PIASxβ and 50 ng of pCHTNS or pCSEOS or pCSEOS125 using the TransIT LT1 Transfection Reagent (Panvera, Madison, WI) as recommended by the manufacturer. After 48 h of transfection, the cells were fixed with 10% formalin in PBS, and permeabilized with 0.2% Triton X-100. The recombinant and truncated NPs were detected using Alexa 647-labeled anti-N MAb. Counter-staining for nucleic DNA was carried out using Hoechst 33342 according to the manufacturer's instructions (Molecular Probes).

3. Results

3.1. Identification of cellular proteins that interact with NP

Yeast two-hybrid screening was carried out using the SEOV NP as bait. Seven positive clones were identified from 1×10^6 library transformants (Table 1). A DNA database search revealed 100% homology with the human PIAS1 (protein inhibitor of activated STAT 1), PIASxβ, TTRAP (TRAF and TNF receptor-associated protein) (Pype et al., 2000), HIPK2 (human homeodomain-interacting protein kinase 2; Kim et al., 1998), CHD3 (chromodomain helicase DNA-binding protein 3; Woodage et al., 1997), and RanBPM (RanGTP-binding protein; Nishitani et al., 2001). It has been reported that PIAS, CHD3, and HIPK2 associate with a number of novel SUMO-1 interacting proteins (Minty et al., 2000). PIAS was reported initially as the Gu/RNA helicase II-binding protein (Valdez et al., 1997), and later as a STAT-1 inhibitor. PIAS1 binds to phosphorylated activated STAT1 dimer in the cytoplasm, and inhibits STAT-mediated gene activation (Liu et al., 1998). More recently, it has been discovered that the PIAS family members possess E3 enzyme activities for sumoylation (Johnson and Gupta, 2001; Kahyo et al., 2001; Takahashi et al., 2001).

Table 1
Identification of cellular proteins that interact with the SEOV NP

Clone number	Coding protein	Accession number	Amino acids
Cl-1	PIAS1	AF167160	284–651
Cl-2	PIAS1	AF167160	159–651
Cl-3	PIASxβ	AF077954	28–621
Cl-4	HIPK2	XM0167072794	474–932
Cl-5	TTRAP	AJ269473	20–362
Cl-6	CHD3	AF006515	1643–1944
Cl-7	RanBPM	AB055311	141–729

These clones were isolated through the yeast two-hybrid screening as pACT2 plasmids that expressed proteins that were fused with the GAL4 AD. All of the plasmids were reacted with pGBT/SEOV 1–429 (entire NP) or pGBT (vector alone). The interactions were measured by the β-galactosidase filter assay. All of the plasmids showed NP-specific interactions (data not shown).

Table 2
Interaction of cellular proteins with Ubc9 and SUMO-1

pACT2	pGBT/Ubc9	pGBT/SUMO-1
PIAS1 (cl-2)	+ + +	+ + +
PIASxβ (cl-3)	+ + +	+ + +
HIPK2 (cl-4)	+ + +	+ + +
TTRAP (cl-6)	+ + +	+ + +
CHD3 (cl-5)	+ +	+ +
RanBPM (cl-7)	–	–

The bait vectors pGBT/Ubc9 and pGBT/SUMO-1 were cotransformed with the prey vectors pACT/PIAS1, pACT/PIASxβ, pACT/HIPK2, pACT/CHD3, pACT/TTRAP, and pACT/RanBPM, which are listed in Table 1. The bait domains (BDs) of Ubc9 and SUMO-1 were assayed for interactions with the prey domains (ADs) of PIAS1, PIASxβ, HIPK2, CHD3, TTRAP and RanBPM using the β-galactosidase assay. The intensity of the interaction, as monitored by β-galactosidase activity, is reported as follows: (–) <5; (+) 5–10; (+ +) 10–50; (+ + +) >50.

3.2. The SUMO-1- and Ubc9-interacting cellular proteins

We investigated the associations between the cellular proteins and sumoylation enzymes. The SUMO-1 and Ubc9 interactions with PIAS 1, PIASxβ, HIPK2, CHD3, TTRAP, and RanBPM were tested in the yeast two-hybrid assay (Table 2). SUMO-1 and Ubc9 (E2 enzyme) showed distinct interactions with PIAS1, PIASxβ, HIPK2, CHD3, and TTRAP, but not with RanBPM. These results confirm that the five proteins that interact with SUMO-1 and Ubc9 are sumoylation-related molecules.

3.3. Determination of the interaction domains of the SEOV and HTNV NPs

As shown in our previous study, the NP–NP interaction was detected in the yeast two-hybrid assay. Although the full-length NP and truncated NP (aa 100–429) showed homotypic interactions, NP 125–429 did not. Two regions (aa 100–125 and aa 403–429) were crucial for homotypic interactions between the NPs. In addition, the tryptophan (W) to alanine (A) alteration at position 119 in the SEOV NP (W119A mutant) led to the loss of the homotypic interaction (Yoshimatsu et al., 2003). To investigate the regions that are responsible for the interactions between cellular proteins and NP, we used a series of truncated NPs (Table 3) in the two-hybrid system. All of the cellular proteins, with the exception of SUMO-1, reacted with the full-length NPs from SEOV and HTNV, SEOV 100–429, SEOV 100–412, and SEOV 1–420, but failed to react with SEOV 125–429 and the W119A mutant of SEOV NP.

3.4. Analysis of the interactions between NP and SUMO-1-related molecules in the mammalian two-hybrid assay

The mammalian cell two-hybrid assay was used to confirm the interactions between the hantavirus NP and cellular proteins. As shown in Fig. 1A left panel, the interactions between NP and the CHD3, HIPK2, TTRAP proteins were confirmed in this assay. However, as shown in right panel of Fig. 1A, NP interactions with PIAS1 and PIASxβ were not observed in both HEK 293 and Hela cells (data not shown). Results from mammalian two-hybrid assay in Hela, Vero, and HEK 293 cells were virtually identical. However, especially in HEK 293 cells, PIAS1 and PIASxβ showed inhibitory effects in the mammalian two-hybrid assay. Therefore, interactions between the PIASs and NP were not detectable in this assay due to the transcription-inhibition activities of the PIAS proteins. The interaction profiles of HIPK2, CHD3, and TTRAP with the truncated NPs were basically the same as those seen in the yeast two-hybrid assay. Although the interaction of CHD3 with truncated NP 100–429 was confirmed, CHD3 did not interact with truncated NP 125–429 (Fig. 1B, left panel). HIPK2 and TTRAP showed basically the same profiles as CHD3 (data not shown). In addition, the homotypic interaction profile in the mammalian two-hybrid assay was the same as that seen in the yeast system. The region that contains aa 100–125 of NP is critical for the NP–NP interaction (Fig. 1B, right panel). These results indicate that the region that is important for the NP–NP interaction is also important for interactions between NP and the SUMO-1-related molecules.

Table 3
Interactions between the hantavirus-truncated NPs and SUMO-1-related molecules

pGBT9	SUMO-1	Ubc9 (E2)	PIAS1 (E3)	PIASxβ (E3)	HIPK2	TTRAP	CHD3	N[a]
SEOV 1–429	–	+ +	+ +	+ +	+ +	+ +	+ +	+ +
SEOV 100–429	–	+ +	+ + +	+ + +	+ + +	+ +	+ +	+ + +
SEOV 125–429	–	–	–	–	–	–	–	–
SEOV 100–412	–	+ +	+ +	+ +	+ +	+ +	+ +	+ +
SEOV W119A	–	–	–	–	–	–	–	–
HTNV 1–429	–	+ +	+ +	+ +	+ +	+ +	+ +	+ +

The bait constructs were prepared in the pGBT9 plasmid vector, as described previously (Yoshimatsu et al., 2003). The prey vectors pGAD424/SUMO-1, pGAD424/Ubc9, pACT2/PIAS1 (clone-2), pACT2/PIASxβ (clone-3), pACT2/HIPK2 (clone-4), pACT2/TTRAP (clone-5), pACT2/CHD3 (clone-6), and pGAD424/SEOV 1-429 were cotransformed with the bait vector into yeast cells. The interactions were measured by the β-galactosidase assay, and the intensity index was derived as described in Table 2.

[a] SEOV NP 1–429.

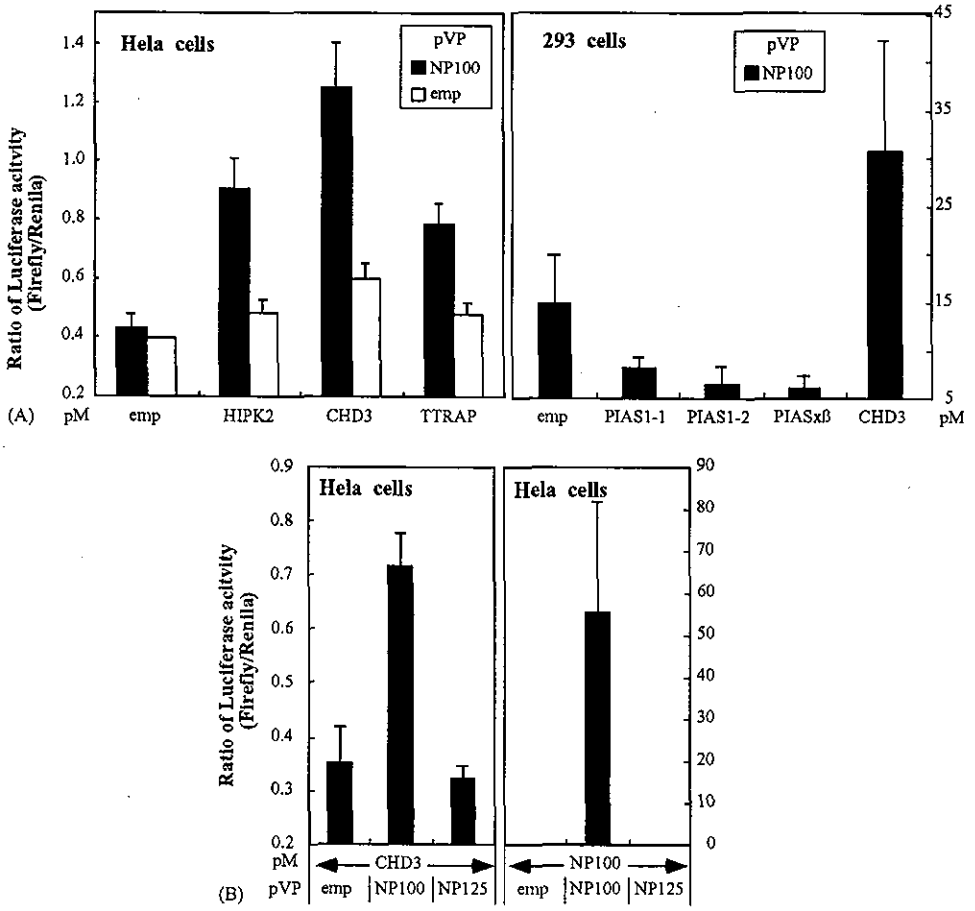

Fig. 1. Interaction between the HTNV NP and SUMO-1-related molecules in mammalian two-hybrid assays. (A) Left panel: interactions between the truncated NP 100–429 (NP100) or pVP vector without an insert (emp) and SUMO-1-related molecules in Hela cells. The interactions between NP and HIPK2, TTRAP, and CHD3 were confirmed. Right panel: interactions between the truncated NP100 and SUMO-1-related molecules in HEK 293 cells. The interactions between NP and the PIAS proteins were not confirmed because of the transcription-inhibition activities of the PIAS proteins. (B) Comparison of the homotypic interactions of NP and interactions between NP and the SUMO-1-related molecules. As shown in the left panel, the binding profiles of NP and CHD3 in Hela cells were generally in accordance with the results of the yeast two-hybrid assay (Table 3). The interaction of CHD3 with the truncated NP 100–429 (NP100) was confirmed. In contrast, neither the truncated NP 125–429 (NP125) nor the pVP vector without an insert (emp) bound to CHD3. HIPK2 and TTRAP showed similar binding profiles to that of CHD3 (data not shown). This profile is in agreement with the homotypic interaction of NP, which is shown in the right panel. NP100 interacted with NP100, but not with NP125 or emp.

3.5. Subcellular localization of NP and PIAS

The localization patterns of NP and PIAS were investigated in Vero E6 cells. The PIASxβ–GFP fusion protein was expressed in Vero E6 cells. PIASxβ was localized mainly in the nuclei (Fig. 2A–C). However, when the SEOV NP and PIASxβ–GFP were co-expressed, the SEOV NP was localized to the cytoplasm (Fig. 2E), and PIASxβ remained in the cytoplasm (Fig. 2D). Similar results were obtained by using HTNV NP (data not shown). Truncated SEOV NP125 did not induce localization change of PIASxβ (Fig. 2G–I). These result indicated that entire HTNV and SEOV NPs were interacted with PIASxβ in cytoplasm and SEOV NP125 was not. These results agreed with results in yeast and mammalian cell two-hybrid assay.

4. Discussion

In this paper, we reported association of hantavirus NP and SUMO-1-related molecules, PIAS1, PIASxβ, HIPK2, CHD3, and TTRAP. Previously, we reported that the HTNV NP interacted with Ubc9 (Maeda et al., 2003). In this study, the HTNV NP interacted with SUMO-1 in the yeast two-hybrid assay based on the LexA system. Kaukinen et al. (2003) also reported that the PUUV NP interacted with SUMO-1 and Ubc9 in a yeast two-hybrid assay that was based on the LexA system. However, reactivity with SUMO-1 was not observed in the present study (Table 3). This discrepancy may be explained by the use of different yeast cell lines and different two-hybrid assay based on GAL4 system, which may have affected sensitivity.

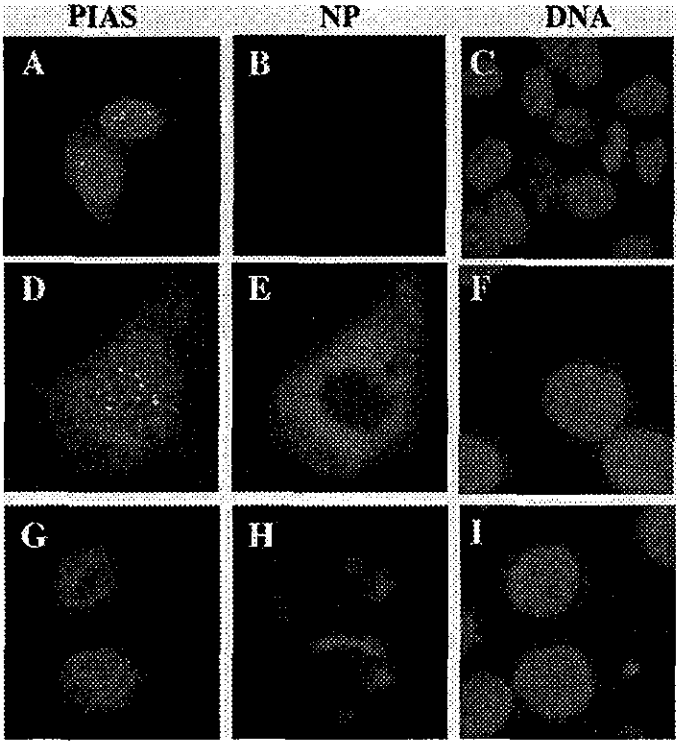

Fig. 2. Subcellular localization of PIAS proteins and SEOV NP. The GFP–PIASxβ fusion was expressed in Vero E6 cells (A–C). Approximately 80% of the expressed PIASxβ were localized to the nuclei using the GFP filter (A), as judged by the Hoechst 33345 DNA staining (C). No signal was observed for the Alexa 647-stained hantavirus NP (B). GFP–PIASxβ and the recombinant SEOV NPs were co-expressed in Vero E6 cells (D—F). Most of the GFP–PIASxβ was distributed in the cytoplasm (D), as was NP (E). The locations of the nuclei were shown by DNA staining (F). GFP–PIASXβ, and the truncated *SEOV NP 125–429* (NP125) were co-expressed in Vero E6 cells (G–I). Most of the expressed GFP–PIASxβ was localized to the nuclei (G), as shown by DNA-staining (I), but the NP125 was localized to the cytoplasm (H).

In a previous report, we determined that the region containing aa 101–238 was essential for NP–Ubc9 interaction (Maeda et al., 2003). As summarized in Table 3, only the constructs that exhibited homotypic interactions showed interactions with the SUMO-1-related molecules. In particular, the aa 100–125 region was critical for this interaction. Furthermore, the W119A mutant, which lost NP multimerization ability, lacked reactivity with PIAS and the SUMO-1-related molecules. These results strongly suggest that the production of the correct NP conformation following multimerization is needed for interactions with the SUMO-1-related molecules.

The interaction profiles of the full-length and truncated NPs seen in the mammalian cell two-hybrid assay basically agreed with those observed in the yeast two-hybrid assay (Table 3). However, the full-length NP showed extremely poor interactions in the mammalian two-hybrid system compared to the yeast system (data not shown). We checked the localization of the fusions between NP and the pVP or pM vector products (data not shown). Interestingly, the pVP-N 1–429 and pM-N 1–429 products were localized mainly to the cytoplasm. Approximately 50% of the pM-N 100–429 product was localized to the nuclei. On the other hand, the pVP-N 100–429 and pVP-N 125–429 products were transported to the nuclei. The pVP vector contains the SV40 nuclear localization signal (NLS) and the pM vector carries GAL4 NLS. Since the full-length NP was incompatible with these NLSs, NP–NP interaction in the nucleus appears to be unlikely.

The localization patterns of PIAS from nuclei to cytoplasms were observed by coexpression of SEOV and HTNV NP. Previously, we reported a similar localization change for Ubc9 when it was co-expressed with NP (Maeda et al., 2003). As shown in Fig. 2D, since the amount of PIASxβ in the nuclei was reduced, the nuclear dot was clearly observed. Nuclear dots may encompass promyelocytic leukemia (PML) nuclear bodies, which are also called PML oncogenic domains or PODs (Sternsdorf et al., 1997). During PUUV infection, NP was reported to be associated with the PML nuclear bodies (Li et al., 2002).

Both the SEOV and HTNV NPs contain the MKAE motif at aa 188–191, which corresponds to the ψKAE (where ψ is a hydrophobic residue) consensus sequence for SUMO-1 modification. In addition, we found that the E2 (Ubc9) and E3 (PIAS) enzymes for sumoylation interacted with SEOV NP and HTNV NP. Based on these findings,

we expected to see sumoylation of the hantavirus NPs. In order to clarify this point, we performed an immunoprecipitation assay. Briefly, the NPs in hantavirus-infected Vero E6 cells were immunoprecipitated with MAb ECO2 in the presence of *N*-ethylmaleimide (an isopeptidase inhibitor), and SUMO-1 that was covalently bound to NP was detected by Western blotting with the anti-SUMO-1 antibody. Unexpectedly, we detected only a poor signal in this assay, despite numerous trials (data not shown). So far, we could not conclude whether or not sumoylation of NP occurs, because no SUMO-1 binding to NP was detected by immunoprecipitaion assay. However, since HTNV and SEOV NPs in infected Vero cells were quite resistant against the solubilization in the immunoprecipitation assay, it was roughly estimated that less than 1% of NP present in the immnoprecipitation assay was actually examined (data not shown). Therefore, if NPs were sumoylated, partially this could not be detected. In addition to the technical difficulty, polymerization dependent interactions of SUMO-1 relating molecules (Table 3) may indicate that sumoylation is also dependent to polymerization. If sumoylation occur only in highly polymerized NP, it would be difficult to detect by ordinary immunoprecipitation assay.

Given that the interactions shown in this and previous reports between hantavirus NP and SUMO-1-related molecules cannot be related to sumoylation, it is interesting to consider alternative roles for these interactions. Increases in the levels of PIAS message were reported in a screen for pathogenetic hantavirus infection-specific host genes using DNA array chips (Geimonen et al., 2002). In addition, PIAS was reported to have transcription-inhibition activity. In the mammalian cell two-hybrid assay, we found that PIASxβ strongly inhibited the positive control for the two-hybrid reaction, which contained a combination of p53 and the SV40 large T antigen (data not shown). Recently, it was reported that members of the PIAS family had transcription-inhibition activities (Coccia et al., 2002; Nishida and Yasuda, 2002). In this respect, Kotaja et al. (2002) reported that transcription inhibition was mediated by the SUMO-1 ligase activity. Further investigations are needed to clarify the role of PIAS in hantavirus infection.

We found that PIAS 1 (28–651), PIAS 1 (284–651), and PIASxβ (full-length) interacted with the hantavirus NP (Fig. 3A). Alignment of these protein sequences showed that the C-terminal portions of the proteins were essential for interaction with NP. PIAS1 and PIASxβ share significant homology in their central regions around the ring-like domain (Liu et al., 1998; Tan et al., 2002). This ring-like domain is conserved among PIAS family members, and is functionally important for SUMO-1 ligase activity (Johnson and Gupta, 2001; Kahyo et al., 2001). This observation suggests that PIAS interacts with the hantavirus NP via this functional region (Fig. 3B).

In general, SUMO-1 conjugation of viral and cellular proteins has been implicated in the regulation of protein–protein interactions, subcellular localization, and stability. There are published reports of four proteins from DNA viruses that are modified by SUMO-1: cytomegalovirus (CMV) IE1 and IE2 (Muller and Dejean, 1999; Hofmann et al., 2000), Epstein–Barr virus (EBV) BZLF1 protein (Adamson and Kenney, 2001), and papillomavirus E1 protein (Yasugi and Howley, 1996). However, information that pertains to a

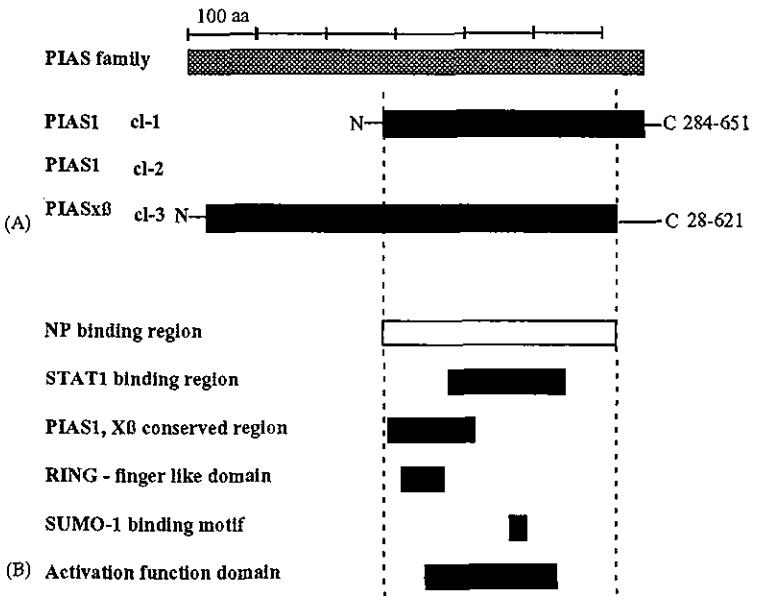

Fig. 3. Functions of the NP-binding region of PIAS1 and PIASxβ. (A) Isolation of three clones from the human kidney cell cDNA library. (B) A schematic representation of the functional domains of PIAS1 and PIASxβ. The PIAS functional domains have been mapped as follows: (1) NP-binding region (this study); (2) PIAS1, PIASxβ conserved region; (3) ring-like domain (Hochstrasser, 2001); and (4) SUMO-1-binding motif (Kotaja et al., 2002).

possible functional role for SUMO-1 modification has not been forthcoming, and to date, no RNA virus proteins have been implicated in sumoylation.

In this paper, we showed that the hantavirus HTNV and SEOV NPs interact with PIAS, Ubc9, and other cellular proteins that are involved in sumoylation. However, unequivocal sumoylation of the hantavirus NP was not detected. Our observations concur with those of a previous report, which showed PUUV NP interactions with SUMO-1 and Ubc9, in the absence of covalent sumoylation (Kaukinen et al., 2003). If the interaction of SUMO-1-related molecules and hantavirus NPs is not linked with sumoylation, the function of these interactions in the virus life cycle remains to be clarified.

Acknowledgements

We would like to thank Dr. H. Yasuda, Tokyo University, Japan for providing the expression plasmid for the GFP–PIASxβ fusion protein. This study was partially supported by grants from the Ministry of Education, Culture, Sports, Science, and Technology of Japan. Textcheck (English language consultants) revised the English in the final draft of this paper.

References

Coccia, E.M., Stellacci, E., Orsatti, R., Benedetti, E., Giacomini, E., Marziali, G., Valdez, B.C., Battistini, A., 2002. Protein inhibitor of activated signal transducer and activator of transcription (STAT)-1 (PIAS-1) regulates the IFN-gamma response in macrophage cell lines. Cell Signal. 14, 537–545.

Desterro, J.M., Thomson, J., Hay, R.T., 1997. Ubch9 conjugates SUMO but not ubiquitin. FEBS Lett. 417, 297–300.

Elliott, R.M., 1990. Molecular biology of the Bunyaviridae. J. Gen. Virol. 71, 501–522.

Geimonen, E., Neff, S., Raymond, T., Kocer, S.S., Gavrilovskaya, I.N., Mackow, E.R., 2002. Pathogenetic and nonpathogenic hantaviruses differentially regulate endothelial cell responses. Proc. Natl. Acad. Sci. U.S.A. 99, 13837–13842.

Gong, L., Li, B., Millas, S., Yeh, E.T., 1999. Molecular cloning and characterization of human AOS1 and UBA2 components of the sentrin-activating enzyme complex. FEBS Lett. 448, 185–189.

Hochstrasser, M., 2001. SP-RING for SUMO: new functions bloom for a ubiquitin-like protein. Cell 107, 5–8.

Johnson, E.S., Gupta, A.A., 2001. An E3-like factor that promotes SUMO conjugation to the yeast septins. Cell 106, 735–744.

Kahyo, T., Nishida, T., Yasuda, H., 2001. Involvement of PIAS1 in the sumoylation of tumor suppressor p53. Mol. Cell. 8, 713–718.

Kaukinen, P., Vaheri, A., Plyusnin, A., 2003. Non-covalent interaction between nucleocapsid protein of Tula hantavirus and small ubiquitin-related modifier-1, SUMO-1. Virus Res.

Kim, Y.H., Choi, C.Y., Lee, S.J., Conti, M.A., Kim, Y., 1998. Homeodomain-interacting protein kinases, a novel family of co-repressors for homeodomain transcription factors. J. Biol. Chem. 273, 25875–25879.

Kotaja, N., Karvonen, U., Janne, O.A., Palvimo, J.J., 2002. PIAS proteins modulate transcription factors by functioning as SUMO-1 ligases. Mol. Cell. Biol. 22, 5222–5234.

Lee, G.W., Melchior, F., Matunis, M.J., Mahajan, R., Tian, Q., Anderson, P., 1998. Modification of Ran GTPase-activating protein by the small ubiquitin-related modifier SUMO-1 requires Ubc9, an E2-type ubiquitin-conjugating enzyme homologue. J. Biol. Chem. 273, 6503–6507.

Li, X.D., Makela, T.P., Guo, D., Soliymani, R., Koistinen, V., Vapalahti, O., Vaheri, A., Lankinen, H., 2002. Hantavirus nucleocapsid protein interacts with the Fas-mediated apoptosis enhancer Daxx. J. Gen. Virol. 83, 759–766.

Liu, B., Liao, J., Rao, X., Kushner, S.A., Chung, C.D., Chang, D.D., Shuai, K., 1998. Inhibition of Stat1-mediated gene activation by PIAS1. Pro. Natl. Acad. Sci. U.S.A. 95, 10626–10631.

Maeda, A., Lee, B.H., Yoshimatsu, K., Saijo, M., Kurane, I., Arikawa, J., Morikawa, S., 2003. The intracellular association of the nucleocapsid protein (NP) of Hantaan virus (HTNV) with small ubiquitin-like modifier-1 (SUMO-1) conjugating enzyme9 (Ubc9). Virology 305, 288–297.

Marmorstein, L.Y., Ouchi, T., Aaronson, S.A., 1998. The BRCA2 gene product functionally interacts with p53 and RAD51. Proc. Natl. Acad. Sci. U.S.A. 95, 13869–13874.

Minty, A., Dumont, X., Kaghad, M., Caput, D., 2000. Covalent modification of p73alpha by SUMO-1. Two-hybrid screening with p73 identifies novel SUMO-1-interacting proteins and a SUMO-1 interaction motif. J. Biol. Chem. 275, 36316–36323.

Miyauchi, Y., Yogosawa, S., Honda, R., Nishida, T., Yasuda, H., 2002. Sumoylation of Mdm2 by protein inhibitor of activated STAT (PIAS) and RanBP2 enzymes. J. Biol. Chem. 277, 50131–50136.

Muller, S., Hoege, C., Pyrowolakis, G., Jentsch, S., 2001. SUMO, ubiquitin's mysterious cousin. Nat. Rev. Mol. Cell. Biol. 2, 202–210.

Nakagawa, Y., Kimura, N., Toyoda, T., Mizumoto, K., Ishihama, A., Oda, K., Nakada, S., 1995. The RNA polymerase PB2 subunit is not required for replication of the influenza virus genome but is involved in capped mRNA synthesis. J. Virol. 69, 728–733.

Nishida, T., Yasuda, H., 2002. PIAS1 and PIASxalpha function as SUMO-E3 ligases toward androgen receptor and repress androgen receptor-dependent transcription. J. Biol. Chem. 277, 41311–41317.

Nishitani, H., Hirose, E., Uchimura, Y., Nakamura, M., Umeda, M., Nishii, K., Mori, N., Nishimoto, T., 2001. Full-sized RanBPM cDNA encodes a protein possessing a long stretch of proline and glutamine within the N-terminal region, comprising a large protein complex. Gene 272, 25–33.

Niwa, H., Yamamura, K., Miyazaki, J., 1991. Efficient selection for high-expression transfectants with a novel eukaryotic vector. Gene 108, 193–199.

Patton, J.T., Davis, N.L., Wertz, G.W., 1984. N protein alone satisfies the requirement for protein synthesis during RNA replication of vesicular stomatitis virus. J. Virol. 49, 303–309.

Pype, S., Declercq, W., Ibrahimi, A., Michiels, C., Van Rietschoten, J.G.I., Dewulf, N., de Boer, M., Vandenabeele, P., Huylebroeck, D., Remacle, J.E., 2000. TTRAP, a novel protein that associates with CD40, tumor necrosis factor (TNF) receptor-75 and TNF receptor-associated factors (TRAFs), and that inhibits nuclear factor-kappaB activation. J. Biol. Chem. 275, 18586–18593.

Saitoh, H., Pu, R.T., Dasso, M., 1997. SUMO-1: wrestling with a new ubiquitin-related modifier. Trends Biol. Sci. 22, 374–376.

Schmaljohn, C., Hjelle, B., 1997. Hantaviruses—a global disease problem. Emerg. Infect. Dis. 3, 95–104.

Schmaljohn, C.S., Dalrymple, J.M., 1983. Analysis of Hantaan virus RNA: evidence for a new genus of Bunyaviridae. Virology 131, 482–491.

Severson, W., Partin, L., Schmaljohn, C., Jonsson, C.B., 1999. Characterization of the Hantaan nucleocapsid protein–ribonucleic acid interaction. J. Biol. Chem. 274, 33732–33739.

Sternsdorf, T., Jensen, K., Will, H., 1997. Evidence for covalent modification of the nuclear dot-associated proteins PML and Sp100 by PIC1/SUMO-1. J. Cell Biol. 139, 1621–1634.

Takahashi, Y., Kahyo, T., Toh, E.A., Yasuda, H., Kikuchi, Y., 2001. Yeast Ull1/Siz1 is a novel SUMO1/Smt3 ligase for septin components and functions as an adaptor between conjugating enzyme and substrates. J. Biol. Chem. 276, 48973–48977.

Valdez, B.C., Henning, D., Perlaky, L., Bush, R.K., Bush, H., 1997. Cloning and characterization of Gu/RH-II binding protein. Biochem. Biophys. Res. Commun. 234, 335–340.

Wilson, V.G., Rangasamy, D., 2001. Viral interaction with the host cell sumoylation system. Virus Res. 81, 17–27.

Woodage, T., Basrai, M.A., Baxevanis, A.D., Hieter, P., Collins, F.C., 1997. Characterization of the CHD family of proteins. Proc. Natl. Acad. Sci. U.S.A. 94, 11472–11477.

Yang, J., Koprowski, H., Dietzschold, B., Fu, Z.F., 1999. Phosphorylation of rabies virus nucleoprotein regulates viral RNA transcription and replication by modulating leader RNA encapsidation. J. Virol. 73, 1661–1664.

Yoshimatsu, K., Arikawa, J., Tamura, M., Yoshida, R., Lundkvist, A., Niklasson, B., Kariwa, H., Azuma, I., 1996. Characterization of the nucleocapsid protein of Hantaan virus strain 76–118 using monoclonal antibodies. J. Gen. Virol. 77, 695–704.

Yoshimatsu, K., Lee, B.-H., Araki, K., Morimatsu, M., Ogino, M., Ebihara, H., Arikawa, J., 2003. The multimerization of hantavirus nucleocapsid protein depends on type-specific epitopes. J. Virol. 77, 943–952.

II 疾患 J 感染症

6. ペットからの感染症

内田幸憲　神戸検疫所長

■念頭におくべき疾患トップテン

平成12年（2000年）に神戸市および福岡市医師会員に行った動物由来感染症（ズーノージス）に関するアンケート調査によると，表1に示した疾患の診察経験が多いことが判明した．特にオウム病，ネコひっかき病，白癬，トキソプラズマ症，サルモネラ症の診察経験が多く，回答医師の23%が何らかのペットからの感染症を経験していた[1]．

近年のペットブームは少子高齢化，核家族化の進行という社会背景のもとに，ペットはコンパニオンアニマル（伴侶動物）として扱われ，人間とペットの共生は緊密化してきている．1974年総理府によって始められた「動物の保護に関する世論調査」を引き継いだ内閣府による「動物保護に関する世論調査」（2002年）[2]では，わが国におけるペット飼育率は36.6%，その内訳は犬62.4%，猫29.2%，魚類11.7%，鳥7.7%，は虫類2.4%，ウサギ2.4%，ネズミ族（齧歯類）2.2%となっている．また，家畜およびイヌ，ネコ，キツネ，スカンク，アライグマ，サルそしてプレリードッグ，コウモリ，ヤマゲネズミ（マストミス），ハクビシン，タヌキ，イタチアナグマの輸入規制以外規制のないわが国では，エキゾチックアニマル（希少動物，珍獣稀獣）の輸入が盛んである．2000年の調査による推計では約380万頭（サル類4600頭，齧歯類110万匹，その他哺乳類3万匹，鳥類60万羽，は虫類200万匹，両生類7万匹など）が輸入されている．これらの動物には野生のものも多く，種々の病原体を保有した動物がペットとして国内にもち込まれている可能性は高い．

表1に示したトップテンの疾患にかかわったペットは，イヌ，ネコ，トリ（オウム，インコ，カナリア，ハトなど）など以前からなじみであったものが多いが，サル，ブタ，チンチラなども少数ながら関与していた．今後，新たな疾患が加わり，ペットからの感染症の増加が懸念される．

表1　念頭におくべき疾患トップテン
（ペット動物由来感染症の診察経験トップテン）

内科系	外科系
1. オウム病	1. ネコひっかき病
2. ネコひっかき病	2. 白癬
3. サルモネラ症	3. トキソプラズマ症
4. クリプトコッカス症	4. (動物咬傷)
5. カンピロバクター腸炎	5. オウム病
6. トキソプラズマ症	6. 犬・猫・ブタ回虫症*2
7. 犬・猫回虫症*1	7. ネコノミ症
8. 疥癬	8. 疥癬
9. 白癬	9. カンピロバクター腸炎
10. パスツレラ症	10. ダニ刺症

*1トキソカラ症（幼虫移行症）を含む
*2眼トキソプラズマ症を含む

■簡潔な医療面接手順

感染症を疑う患者にはペット動物の関与を意識して以下の問診を行うことが望まれる．

①発熱，呼吸器症状，消化器症状などの状況とその出現の経時的な変化

②ペット動物の飼育の有無，その種類および飼育の仕方（室内か否か，接触の程度・頻度）

③生活圏でのペット動物などとの接触状況（職業: ペットショップ勤務・動物病院勤務・調理師など，砂場遊びの有無，生活環境: 老人ホーム・保育園でのペット飼育の有無）

④感染源と推定される動物の健康状態

⑤同居者など感染源と思われるペット動物との接触者の健康状態

診察所要時間のこともあるが，丁寧な問診の有